Collective relaxation processes in atoms, molecules and clusters

2016 J. Phys. B: At. Mol. Opt. Phys. 49 082001

(http://iopscience.iop.org/0953-4075/49/8/082001)

IOP Publishing Journal of Physics B: Atomic, Molecular and Optical Physics
J. Phys. B: At. Mol. Opt. Phys. **49** (2016) 082001 (18pp) doi:10.1088/0953-4075/49/8/082001

Topical Review

Collective relaxation processes in atoms, molecules and clusters

Přemysl Kolorenč[1], Vitali Averbukh[2], Raimund Feifel[3] and John Eland[3,4]

[1] Charles University in Prague, Faculty of Mathematics and Physics, Institute of Theoretical Physics, V Holešovičkách 2, 18000 Prague, Czech Republic
[2] Department of Physics, Imperial College London, Prince Consort Road, SW7 2AZ London, UK
[3] Department of Physics, University of Gothenburg, Origovägen 6B, SE-412 96 Gothenburg, Sweden
[4] Department of Chemistry, Physical & Theoretical Chemistry Laboratory, Oxford University, South Parks Road, Oxford OX1 3QZ, UK

E-mail: kolorenc@mbox.troja.mff.cuni.cz

Received 6 February 2015, revised 26 February 2016
Accepted for publication 2 March 2016
Published 4 April 2016

Abstract

Electron correlation is an essential driver of a variety of relaxation processes in excited atomic and molecular systems. These are phenomena which often lead to autoionization typically involving two-electron transitions, such as the well-known Auger effect. However, electron correlation can give rise also to higher-order processes characterized by multi-electron transitions. Basic examples include simultaneous two-electron emission upon recombination of an inner-shell vacancy (double Auger decay) or collective decay of two holes with emission of a single electron. First reports of this class of processes date back to the 1960s, but their investigation intensified only recently with the advent of free-electron lasers. High fluxes of high-energy photons induce multiple excitation or ionization of a system on the femtosecond timescale and under such conditions the importance of multi-electron processes increases significantly. We present an overview of experimental and theoretical works on selected multi-electron relaxation phenomena in systems of different complexity, going from double Auger decay in atoms and small molecules to collective interatomic autoionization processes in nanoscale samples.

Keywords: electron correlation, autoionization, multiple ionization

(Some figures may appear in colour only in the online journal)

1. Introduction

Multi-electron relaxation processes are of fundamental importance for the understanding of correlation in bound systems. Their study was stimulated for instance in connection with the decay of the so-called hollow atoms, which can be produced in the course of neutralization of slow highly charged ions at surfaces [1, 2] or upon irradiation of matter by high-intensity x-ray free-electron lasers (FELs) [3]. The interaction between intense, high-energy light pulses and matter has become a very active field of research and one of today's most exciting topics in atomic and molecular science. At high power densities a large molecule or cluster can absorb a large number of photons, triggering the system to undergo a transition to a highly excited state. Ionization is in this case strongly interlinked with correlated electron dynamics, either due to multielectron collisions with energy exchange or by autoionization processes related to interatomic Coulombic decay (ICD), in which the energy acquired from relaxation of a vacancy on one cluster constituent is transferred to a neighbor and utilized for its ionization [4].

What can possibly be considered as the first report of a three-electron relaxation process was presented by Carlson and Krause in 1965 [5] who provided experimental evidence for double Auger decay (DAD), in which two electrons are emitted upon relaxation of a single inner shell vacancy, see

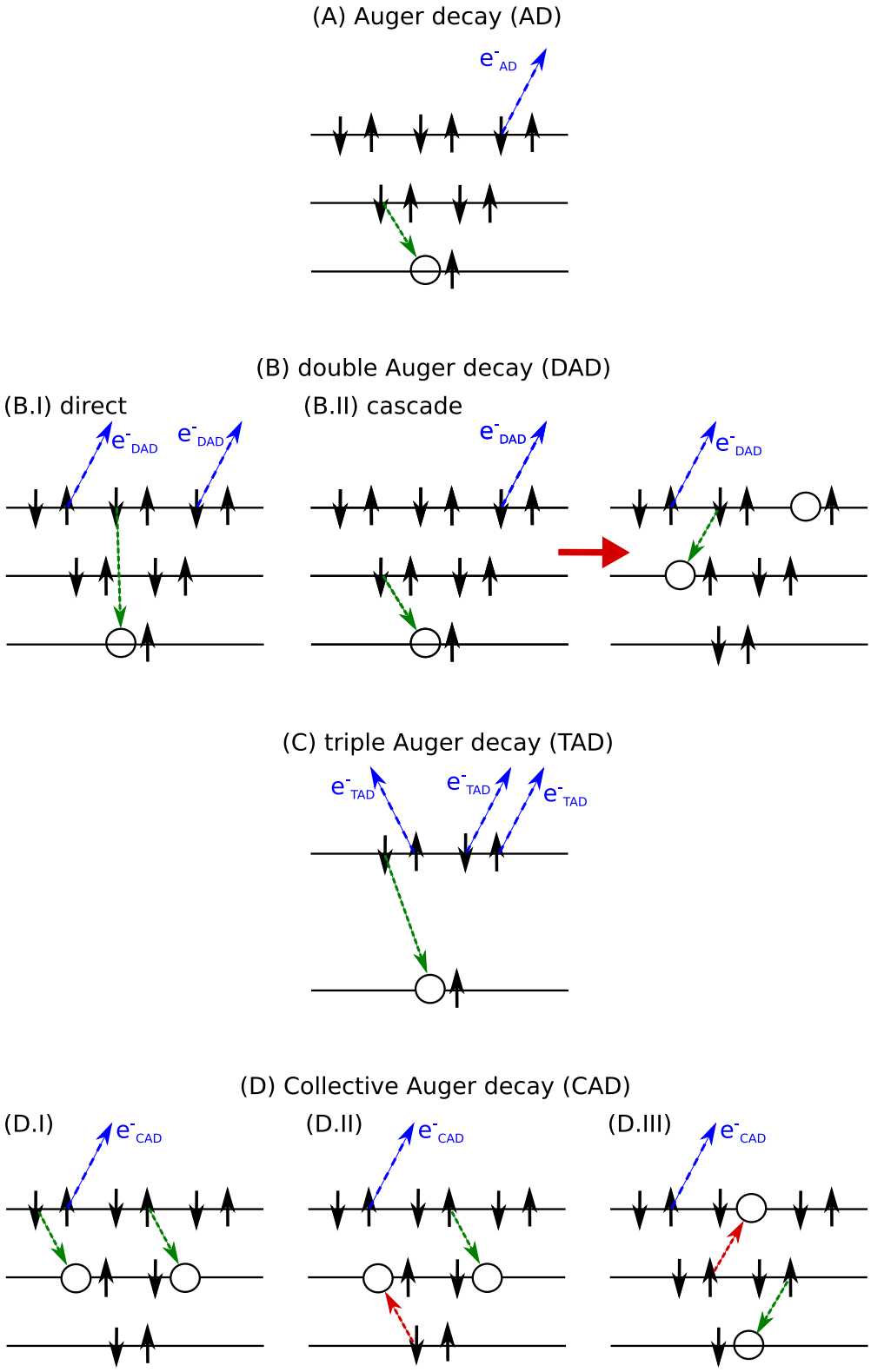

Figure 1. Two-electron Auger decay (A) and related intraatomic multi-electron decay processes: (B) double Auger decay (direct and cascade transitions); (C) triple Auger decay; (D) collective Auger decay (in transitions D.II and D.III, the energy gained from the recombination of a single vacancy is distributed between two electrons, leading to the emission of a less energetic electron as compared to D.I).

figure 1(B). DAD emission may occur in two different ways. In direct DAD (figure 1(B.I)), the two electrons are ejected simultaneously and share the excess energy continuously with a pronounced preference of a U-shaped energy sharing distribution that corresponds to the emission of one slow and one fast electron. In contrast, cascade DAD in which the two electrons are emitted sequentially (figure 1(B.II)) gives rise to a structured energy spectrum—each electron has a discrete

energy given by the energy difference between the initial, intermediate and final states involved in the relaxation cascade. A number of theoretical and experimental studies have been devoted to DAD in both atomic and molecular systems, and they show that the contribution of the direct DAD driven by three electron correlation can indeed be significant [6, 7 and references therein].

Another kind of three electron process is collective Auger decay (CAD) in which two inner-shell vacancies are simultaneously filled by outer-shell electrons and a third electron is ejected into the continuum[5]. Various CAD transitions are shown in figure 1(D). An analogous radiative process, in which a double vacancy is filled by two electrons and a single photon is emitted is also known [8–10]. CAD was probably first observed in 1975 by Afrosimov *et al* [11] in collisions of various ions with Ar atoms. More convincing experimental evidence was given by Lee *et al* [12] in the case of resonantly excited Kr and by De Filippo *et al* in highly charged carbon atoms [13]. Theoretically, the CAD process is well understood in atoms [9, 14]. The efficiency of CAD is usually very small, the branching ratio (BR) of CAD relative to normal two-electron Auger decay (AD) ranging from 10^{-4} to 10^{-6}. The larger value is attained most often in low-Z atoms where 2s → 1s shake-down processes dominate the relaxation due to the nonorthogonality of initial 2s and final 1s wave functions [15]. In high-Z atoms this effect is much less significant and CAD is driven purely by three-electron correlation, leading to a substantial drop in efficiency. Compatible ratios were observed for the cross sections of di- and trielectronic recombination, which represent time-reversed processes related to normal and CAD, respectively. The cross sections are therefore connected to the Auger rates by the principle of detailed balance [16, 17].

Although CAD in atomic systems has been found to be extremely weak, under favorable conditions the three-electron relaxation processes can become dominant decay channels. An example of such a case is double inner-valence ionization in molecules. For instance, the energy of doubly F(2s) ionized fluoromethane is well above the triple-ionization threshold but all decay channels with at least one F(2s) vacancy are energetically closed. Therefore, collective decay of the two initial vacancies represents the only accessible nonradiative relaxation pathway. Recent *ab initio* calculations [18] predicted a surprisingly short lifetime of about 3 fs, which is well within the range of typical two-electron AD. Excellent agreement of the calculated and measured electron spectra provides experimental support for this rather astonishing result [18].

Over the last two decades, interatomic decay processes such as ICD (see figure 2(A)) have been studied intensively both theoretically and experimentally in weakly bound van der Waals or hydrogen-bonded clusters [19–21]. Related collective decay processes of multiply inner-valence ionized or excited clusters were recently proposed and observed experimentally [22–24]. Despite the significantly weaker

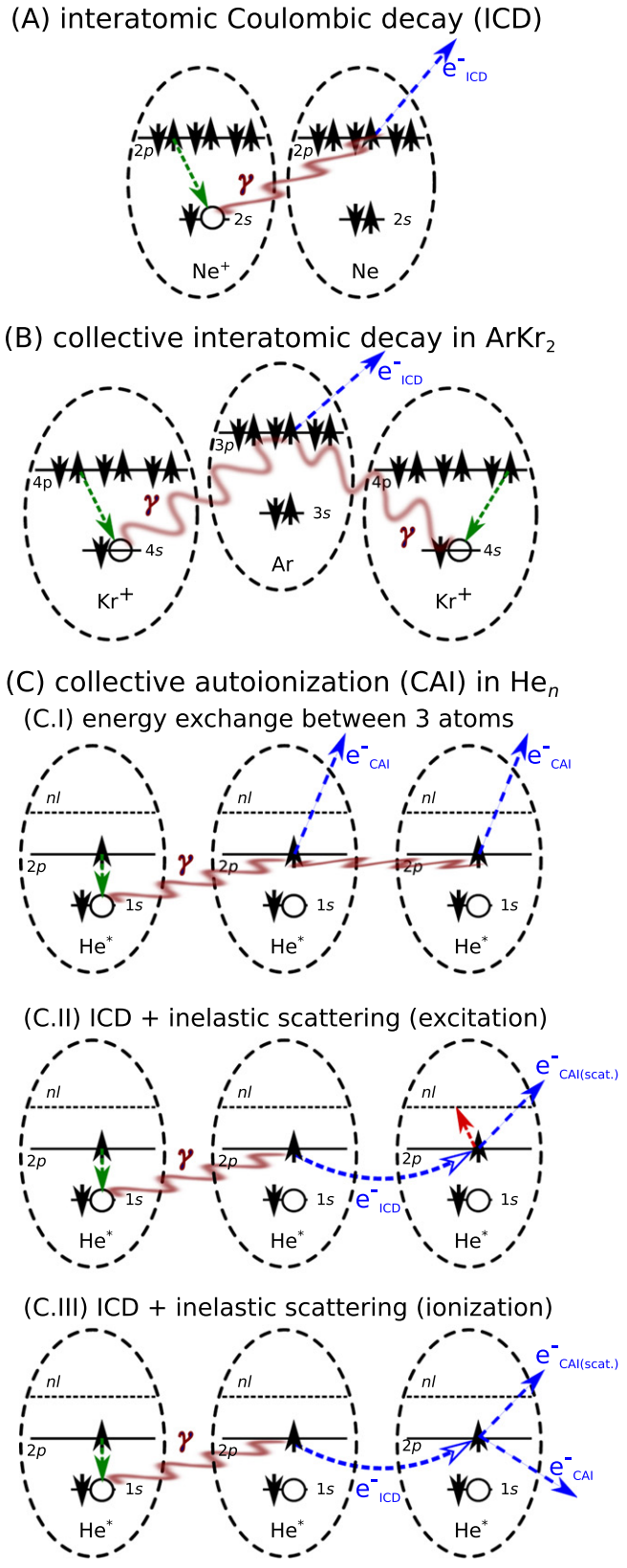

Figure 2. Two-electron interatomic Coulombic decay (A) and related interatomic multi-electron decay processes: (B) collective interatomic decay of two inner-shell vacancies in a mixed Kr–Ar cluster; (C) collective autoionization in multiply excited helium cluster.

[5] In existing literature, this relaxation transition is often termed DAD, which may cause confusion with the previously discussed process.

interatomic correlation in van der Waals clusters as compared to molecules, it has been shown that higher-order decay pathways can play an important role, particularly if the two-electron radiationless decay channels are closed. Even the dissociative dynamics induced by multiple ionization cannot fully quench the multi-electron relaxation. Very recently, interatomic collective autoionization (CAI) processes have been shown to play a dominant role in resonantly irradiated helium clusters due to formation of a collectively excited plasma-like state [25, 26].

Section 2 of the present review is devoted to the DAD in atoms and molecules and covers in detail both theoretical and experimental advances in the field. Short account on the recently observed triple Auger decay (TAD) is given in section 3. CAD in atoms and molecules is discussed in sections 4 and 5, followed by a survey of multi-electron relaxation phenomena in clusters.

2. Double Auger decay

Of the multi-electron processes presented in the introduction, DAD is the most thoroughly studied representative. Even though the process is, of course, less probable than the ordinary single AD, it nevertheless accounts for a sizable fraction of all relaxation processes of inner-shell vacancy states. Therefore, it constitutes a practically accessible source of information about multi-electron correlations. It is particularly the direct double Auger process, in which both electrons are ejected simultaneously, that is of interest in this context. In the present section, we first review the theoretical description of DAD based on the many body perturbation theory (MBPT). It provides an intelligible physical picture of different mechanisms contributing to DAD and also guidance for distinguishing between them by experiment. Then, an overview of available experimental and theoretical results on DAD in different atomic and molecular systems is given.

2.1. Theory of double Auger decay

Already in the pioneering work of Carlson and Krause [5] an attempt was made to explain the observed DAD signal in terms of electron shake-off, a transition induced by changes in the effective charge. In this process, the primary Auger electron is ejected rapidly after inner hole recombination and a subsequent transition of the secondary electron to the continuum takes place due to the alteration of the atomic potential. The probability of an electron vacating the nl orbital due to a sudden change of effective charge by $\Delta Z_{\rm eff}$ can be estimated from the formula

$$P_{\rm nl} = 1 - |\langle\psi_{\rm f}|\psi_{\rm i}\rangle|^2, \tag{1}$$

where $\psi_{\rm i}$ is the initial one-electron wave function of the nl electron in the field of an effective charge $Z_{\rm eff}$ and $\psi_{\rm f}$ is its final wave function for an effective charge $Z_{\rm eff} + \Delta Z_{\rm eff}$. It was immediately obvious that shake-off cannot fully explain DAD. For the Ne K vacancy, the calculations gave an upper limit of 0.5% for the shake-off probability while the measured relative abundance of Ne^{3+} was 8% [5]. Later theoretical calculations in which shake-off was considered as the only DAD mechanism also strongly underestimated the observed probabilities (see, e.g., [27]).

The first calculation of DAD rates in the framework of MBPT beyond the shake-off model was performed by Simons and Kelly for the double 1s hole state of neutral lithium [28]. More detailed analysis of the DAD transition amplitudes was performed by Amusia and coworkers in a seminal work [29]. Three fundamental mechanisms contributing to the decay were revealed—the sequential (cascade) pathway, simultaneous emission via shake-off and knock-out. The separation of shake-off and knock-out mechanisms was exploited by Zeng *et al* [7, 30] to develop a practical method for the evaluation of direct DAD rates, which utilizes the distorted wave approximation and a large-scale configuration interaction description of the successive ions.

In first order perturbation theory, the single AD rate is given by

$$A^1_{\rm im} = \frac{4}{k_{\rm m}} |\langle\Psi^+_{\rm m}|V|\Psi_{\rm i}\rangle|^2, \tag{2}$$

where $|\Psi_{\rm i}\rangle$ is the initial autoionizing level of the ion with charge q and $|\Psi^+_{\rm m}\rangle$ is the momentum-normalized final continuum state of an ion with charge $q + 1$ with an electron in the continuum. $k_{\rm m}$ is the momentum of the Auger electron and V is the two-electron interaction potential (Coulomb operator). Energy conservation $\epsilon_{\rm i} = \epsilon^+_{\rm m} + k^2_{\rm m}/2$ is implied. The rate of a cascade DAD can be evaluated by subsequent application of the above formula for each cascade step as [29]

$$A^{\rm cascade}_{\rm if} = \hbar \sum_{\rm m} \frac{A^1_{\rm im} A^1_{\rm mf}}{\Gamma_{\rm m}}, \tag{3}$$

where $\Gamma_{\rm m} = \hbar \sum_{\rm f} A^1_{\rm mf}$ is the total decay width of the intermediate level $|\Psi^+_{\rm m}\rangle$. The summation runs over intermediate energy levels of sufficiently long lifetime so that the physical interpretation of sequential electron emission is meaningful. The energy conservation law holds in each decay step, leading to a discrete energy distribution between the two Auger electrons, and thereby to an electron spectrum which shows distinct lines corresponding to energy differences between the initial and intermediate and between the intermediate and final ionic levels.

For the study of multi-electron correlation, simultaneous ejection of both Auger electrons is the more relevant mechanism. Direct DAD rates can be calculated in second order perturbation theory as [30, 31]

$$A^2_{\rm if} = \frac{8}{\pi} \int_0^{k_{\rm max}} \frac{{\rm d}k_{\rm f1}}{k_{\rm f2}} \left| \sum_{\rm m} \not\int_{k_{\rm m}} \frac{\langle\Psi^{2+}_{\rm f}|V|\Psi^+_{\rm m}\rangle \langle\Psi^+_{\rm m}|V|\Psi_{\rm i}\rangle}{\epsilon_{\rm i} - \epsilon^+_{\rm m} - k^2_{\rm m}/2} \right|^2. \tag{4}$$

Here, $|\Psi^{2+}_{\rm f}\rangle$ is the final state of an ion with charge $q + 2$ with two continuum electrons and $|\Psi^+_{\rm m}\rangle$ defined above now plays the role of a virtual intermediate state. The energy conservation reads $\epsilon_{\rm i} = \epsilon^{2+}_{\rm f} + k^2_{\rm f1}/2 + k^2_{\rm f2}/2$ with $k_{\rm f1}$ and $k_{\rm f2}$ being the momenta of the two Auger electrons. To avoid double counting of the continuum states, the upper integration limit is set to $k_{\rm max} = \sqrt{k^2_{\rm f1}/2 + k^2_{\rm f2}/2}$. It corresponds to an upper

limit $E_{max}/2$ in an integration over the energy with $E_{max} = \epsilon_i - \epsilon_f$. The summations over intermediate states $|\Psi_m^+\rangle$ include summation over all possible $(q + 1)$ ion levels and a summation/integration over a complete set of bound and continuum states of the remaining electron. The vanishing denominator $D = \epsilon_i - \epsilon_m^+ - k_m^2/2$ is treated in the usual way using

$$\lim_{\eta \to 0}(D + i\eta)^{-1} = \mathcal{P}D^{-1} - i\pi\delta(D), \tag{5}$$

where $\mathcal{P}$ stands for the principal-value integration.

Direct evaluation of the expression (4) is extremely complex. To simplify the calculations, two approximate formulae can be derived which correspond to the shake-off and knock-out mechanisms, respectively. In the case of shake-off-driven transition, the direct DAD rate can be decomposed into the formula

$$A_{if}^{SO} = \sum_m A_{im}^1 \, |\langle \Psi_f^{2+} | \Psi_m^+ \rangle|^2, \tag{6}$$

where A_{im}^1 is the single AD rate from the initial hole level i to an intermediate level m. Since the shake-off picture relies on the sudden approximation, it properly describes direct DAD in the high-energy limit of the (primary) Auger electron. In this limit, practical evaluation of the overlap integral in formula (6) is further simplified since the first Auger electron need not be considered. In contrast to cascade DAD, the shake-off process leads to continuous energy sharing between the two outgoing electrons, i.e., each of the electrons may have any kinetic energy between 0 and E_{max}. It can be shown that the most probable energy distribution is strongly asymmetric with one fast and one slow electron [29]. The higher probability of 'shaking' of a slow electron rather than a fast one can be easily deduced from equation (6) since the overlap integral between the continuum wave function of the outgoing (secondary) Auger electron and a bound electron orbital decreases rapidly with increasing energy of the emitted electron.

At a lower electron energy the knock-out mechanism, also referred to as virtual inelastic scattering, usually prevails. It corresponds to a situation where the imaginary part of equation (5) dominates the direct DAD transition amplitude. Neglecting the real part, the formula for the knock-out rate simplifies to [30]

$$A_{if}^{KO} = \sum_m A_{im}^1 \Omega_{mf}(\epsilon_{im}), \tag{7}$$

where $\Omega_{mf}(\epsilon_{im})$ is the dimensionless electron impact collision strength. It is related to the inelastic scattering cross section σ_{mf} of the 'intermediate' Auger electron from the middle level m to the final level f as (see, e.g., [32])

$$\Omega_{mf}(\epsilon) = \frac{g_m k^2}{\pi a_0^2} \sigma_{mf}(\epsilon). \tag{8}$$

Here, g_m is the statistical weight of the intermediate state $|\Psi_m^+\rangle$ and k is the momentum of the incident electron. Formula (7) directly suggests a physical picture of the knock-out mechanism. An Auger electron is emitted with an energy ϵ_{im} which satisfies the energy conservation law for a transition from the initial level i to an intermediate level m. This electron collides inelastically with another outer-shell electron, which is also ejected to the continuum. This interpretation is further supported by the analysis of Simons and Kelly [28], who showed that the imaginary contribution to the DAD transition amplitude is at the expense of the single AD rate. Indeed, some decay events which begin as single AD contribute to DAD due to the subsequent electron collisions. In the case of knock-out, the energy sharing between the two electrons is again continuous, but is determined by the collision process. As in the case of shake-off, there is a preference for one fast and one slow electron. However, the knock-out energy spectrum is typically flatter in comparison with the pronounced U-shape of the shake-off one [33, 34].

Independent evaluation of the shake-off and knock-out rates by means of equations (6) and (7), respectively, neglects interference between the two mechanisms. Such an assumption is certainly justified if one contribution dominates, which is the case of, e.g., the decay of the Ar 2p vacancy [7]. For other systems such as Kr 3d the situation might be more complicated due to the comparable strength of both contributions [30]. However, studies of single-photon double photoionization suggest that the two mechanisms can be separated rather generally, possibly because of the quasi-classical nature of knock-out contrasted with the purely quantum character of shake-off [33, 35].

Two-electron angular correlation patterns in DAD were studied theoretically by Amusia *et al* [29] and by Grum-Grzhimailo and Kabachnik [36]. The analysis revealed an important difference between simultaneous and cascade emission mechanism. The angular distribution of cascade Auger electrons contains only even spherical harmonics [37, 38]. It implies that the angular correlation pattern shows not only axial symmetry with respect to the direction of emission of the first electron but also a forward–backward symmetry. In the case of simultaneous process, this symmetry can be broken by the occurrence of a minimum in the back-to-back emission for near equal energy sharing between the two electrons [29, 36]. These properties were indeed observed in rare gas atoms by Viefhaus and collaborators [39, 40].

2.2. Double Auger decay in rare gases

For a review of early studies on DAD see [41]. The first experimental observations of DAD were based on measuring the ion yield following core ionization of different rare gases [5, 42–46]. These experiments showed significant relative abundances of ionic states of charges larger than two, making the rare gas atoms suitable candidates for further studies of DAD. Subsequent measurements utilized electron–ion [47–51] or electron–electron [39, 40, 52–59] coincidence techniques. These advanced approaches allowed for disambiguation between cascade and direct DAD, utilizing the distinct characters of electron energy distributions.

For the Ne 1s core vacancy, the pioneering work of Carlson and Krause [5] gave the BR of DAD to the total decay rate as 8%. Later measurements refined the value to 6% [46, 49]. In these two experiments, TAD to Ne^{4+} was also

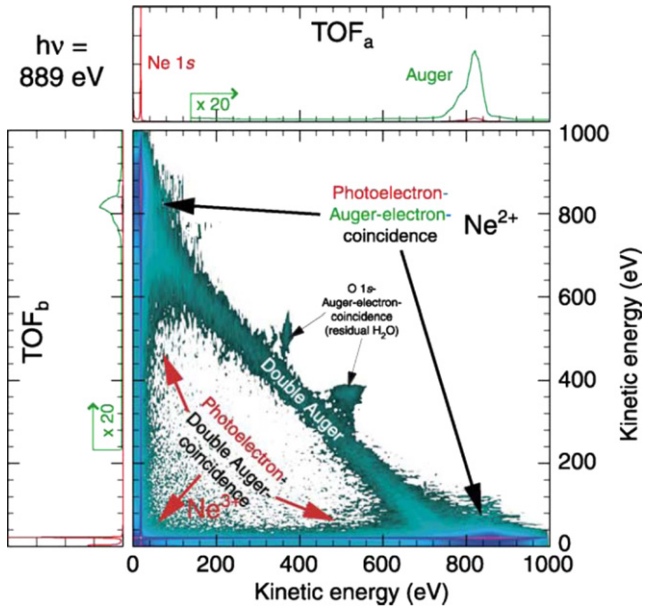

Figure 3. Two-dimensional electron–electron coincidence spectrum of Ne taken at the photon energy $h\nu = 889$ eV along with two corresponding noncoincidence spectra. Structures due to normal Auger decay are marked by Ne^{2+}. Diagonal stripes in which the sum of the kinetic energies is constant are caused by the double Auger electrons. Reprinted from [40], Copyright 2004, with permission from Elsevier.

detected, with a BR of approximately 0.3%. Viefhaus and coworkers [40] studied DAD in Ne by means of angle-resolved time-of-flight electron–electron coincidence spectroscopy. Although the DAD BR is not given by the authors, the approach makes it possible to distinguish the direct and cascade decay pathways, based on the distinct character of the respective energy spectra. For Ne, the measured coincidence spectrum shown in figure 3 exhibits continuous energy sharing between the two electrons, demonstrating that the DAD is dominated by the direct process. Discrete structures characteristic of the decay cascades are completely missing.

Further insight into DAD in Ne is provided by Hayaishi *et al* [60] who performed an electron–ion coincidence study of resonant DAD of the $1s^{-1}3p$ resonance in Ne. The measured Ne^{2+} ion yield corresponding to resonant DAD was 33%, but in contrast to core-ionized Ne, decay cascades are available for relaxation of the studied resonance. Coincidence with threshold electrons made it possible to isolate the contribution of the direct decay pathway with a BR of 6%. The similarity of the direct double Auger BR for the core-ionized and core-excited states indicates that the process is dominated by the knock-out mechanism. This conclusion is based on the reasoning that excited electrons are more susceptible to shake-off than valence electrons. Therefore, if the shake-off mechanism contributed significantly to the direct DAD of the Ne(1s) hole state, the efficiency would increase in the presence of the excited 3p electron through the participator decay process. In the knock-out mechanism, the probability of the primary Auger electron to collide with valence electrons is higher than with the excited electron, which occupies a more diffuse virtual or Rydberg orbital. Therefore, this mechanism involves predominantly the valence electrons (spectator decay) and the presence of the additional 3p electron does not significantly affect the probability of the decay process.

The experimental BR of 6% is in good agreement with the latest theoretical value of 5.39% calculated by Kochur *et al* [61] by means of configuration interaction including both core-core and core-Auger electron correlations. Similar configuration interaction-based calculations of Kanngiesser and coworkers [49] included smaller numbers of configurations and completely neglected the core-Auger electron correlation, leading to an underestimated BR of 3%. Other available theoretical BR values include 0.5% estimated by Carlson and Krause [5] considering solely the shake-off mechanism and 4% calculated by Amusia *et al* [29] using MBPT theory. However, in the latter work, only the decay rate to the $2s^{-2}2p^{-1}$ channel was evaluated and the total DAD BR was then estimated assuming uniform decay rates for the other relevant channels. The extremely small value obtained by Carlson and Krause further confirms the dominance of the knock-out mechanism.

Before moving to heavier rare gas atoms, it is interesting to note that signal attributed to DAD with a BR of about 1% was also observed by Kreidi and coworkers [62] in a cold target recoil ion momentum spectroscopy (COLTRIMS) study of relaxation processes following 1s photoionization in neon dimer. The COLTRIMS method makes it possible to detect in coincidence the two Ne ions originating from Coulomb explosion of two-site di- or tricationic states of the dimer and to extract a complete kinematic description of the decay event. Only the $K - L_{2,3}L_{2,3}L_{2,3}$ DAD channel is observed in the experiment because it leads to asymmetric breakup through radiationless charge transfer. The charge transfer occurs due to nonadiabatic coupling between the one-site $Ne^{3+}(2p^{-3})$-Ne states, populated by DAD of the core hole atomic state, and two-site tricationic states $Ne^{2+}(2p^{-2})$-$Ne^{+}(2p^{-1})$. The measured BR is in reasonable agreement with the $K–L_{2,3}L_{2,3}L_{2,3}$ partial DAD rate of 1.64% calculated by Kanngiesser *et al* [49].

For Ar 2p core vacancy states, the experiments based on ion yield measurements indicated a BR of DAD relative to total decay rates around 10% [42, 45, 46]. This value was also confirmed by the electron–ion coincidence experiment of Saito and Suzuki [48]. More recent experiments favor a slightly higher BR of 13%–15% [40, 50, 59]. However, the discrepancies do not significantly exceed the stated experimental uncertainties. The contributions from direct and cascade processes were determined from multi-electron coincidence experiment by Viefhaus *et al* [40] as 9.6% and 3.4%, respectively. These results are in very good agreement with the calculations of Zeng *et al* [7] who applied equations (6), (7) and (3) to determine the direct and sequential DAD decay rates. Using large-scale relativistic configuration interaction calculations in combination with the distorted wave approximation, they obtained 12.0% and 2.9% for the direct and cascade DAD BR, respectively. As in the case of Ne 1s decay, direct DAD is found to be dominated by the knock-out mechanism. The calculated shake-off

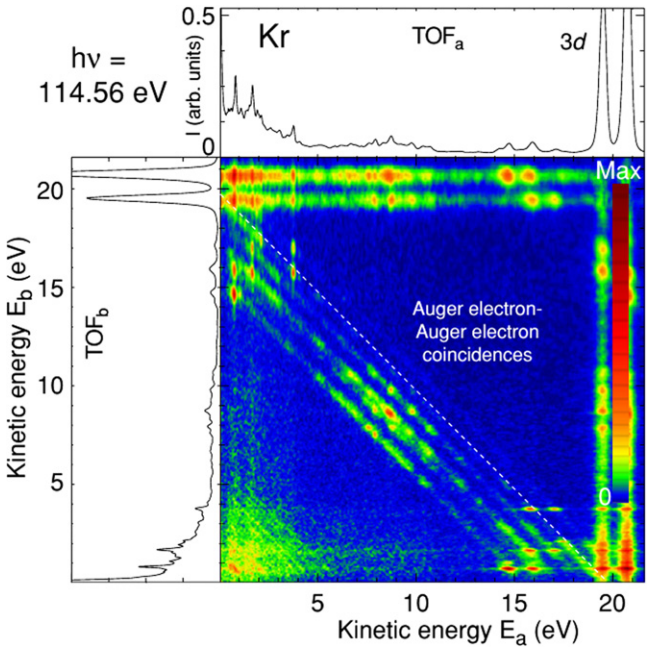

Figure 4. Low energy region of the coincidence map after photoionization of the Kr 3d shell (photon energy $h\nu = 114.56$ eV) together with two noncoincident spectra. Reproduced with permission from [53], Copyright 2004 IOP Publishing Ltd.

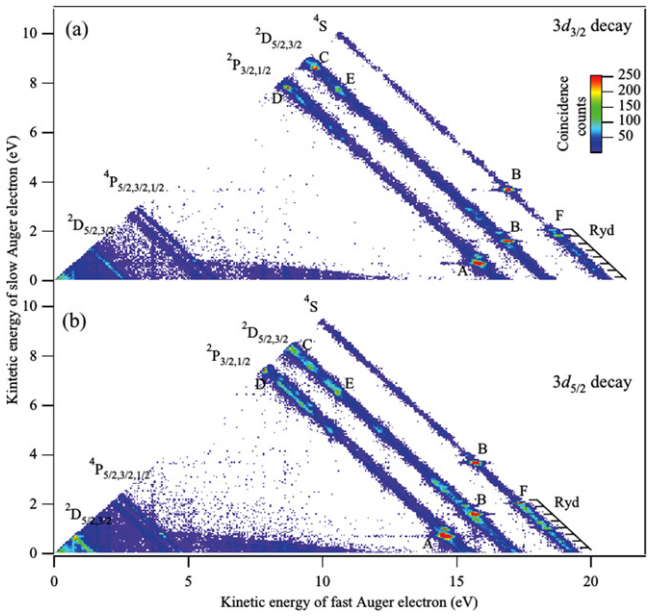

Figure 5. Energy correlations between two Auger electrons after photoionization of the Kr atom detected in coincidence with a $3d_{3/2}$ photoelectron (a) or a $3d_{5/2}$ photoelectron (b). Counts (represented by colors) are given on a linear scale. The capital letters indicate the contribution of different intermediate Kr^{2+} states, involved in cascade Auger decay. The states are labeled according to their intensity (i.e., A is the most intense; F is the weakest). Reproduced with permission from [57], Copyright 2010 American Physical Society.

probability is only 0.6% in excellent agreement with the early estimate by Carlson and Krause [42]. This result also justifies an independent evaluation of the two contributions to the direct decay pathway. Even in the strongest channels, the shake-off to knock-out ratio does not exceed 7%, which can be used as an upper estimate of the influence of interference between the two mechanisms. As in the case of Ne, the dominant role of knock-out is further confirmed by the spectator character of the resonant DAD of 2p core-excited Ar [34].

Going from Ar 2p to Kr 3d ionization, the DAD BR increases to about 25%–30% [35, 46, 48, 50, 51, 63]. In sharp contrast to the lighter Ne and Ar atoms, the relaxation is found to proceed almost exclusively by cascade decay [53, 57, 58]. This is demonstrated in figure 4, where the diagonal stripes are dominated by intense discrete spots. This observation is in notable contradiction with the calculations of Zeng *et al* [30]. Using the same approach as for Ar, they obtained for the cascade and direct DAD BRs similar values, namely 16.6% and 16.5%, respectively. Surprisingly, this accounts for the total DAD BR of 33.1%, which is in satisfactory agreement with the measured value.

The picture of DAD of the Xe 4d vacancy is similar to that of Kr 3d. The measured DAD BR of 20% [46–48, 54] is lower, but the decay is again dominated by the cascade process [52–54, 64]. Penent *et al* [54] investigated the cascade in detail using multielectron spectroscopy with a magnetic bottle spectrometer and showed that the dominant path is rapid (6 fs) ejection of a slow Auger electron followed by the emission of a faster second electron within about 23 fs. Post-collision interaction in the two-electron emission was studied by Lablanquie and coworkers [52]. On the basis of the theoretical results of Sheinerman and Koike [65–67], the observed line shapes distortions further confirm the cascade character of the decay with initial emission of the slower electron. From the analysis of the second Auger electron line shapes the lifetimes of the intermediate states were estimated to be about 11 fs. Recently, in-depth investigation of post-collision interaction in DAD of Ar 2p and Kr 3d vacancies through a combined theoretical and experimental approach was conducted by Sheinerman and coworkers [68–70].

From the existing literature it is not possible to draw any definitive conclusion about the disagreement between theory and experiment concerning the contribution of direct DAD to the decay of the Kr(3d) vacancy state. However, it is noted by Viefhaus *et al* [53] that despite the high resolution of the most recent experiments, the data usually cannot completely rule out that the observed discrete lines corresponding to cascade DAD are superimposed on continuously distributed electron intensity originating in direct DAD. Figure 5 represents a particularly illustrative example of the problem. To help solving it, angle-resolving capabilities of multi-electron coincidence measurements have been employed as an alternative way to distinguish between the direct and cascade pathways. As discussed in section 2.1, the forward–backward symmetry of the two-electron angular correlation patterns can be broken in the case of simultaneous emission. However, no such breakdown was found in the Kr(3d) or Xe(4d) DAD spectra [53], in sharp contrast to DAD of Ne(1s) and Ar(2p)

vacancy states with prevailing simultaneous emission [39, 40].

2.3. Lithium-like atoms

Besides rare gases, the lithium atom, notably the $Li^*(2s^22p\ ^2P^0)$ hollow resonance state at 142.3 eV excitation energy, is another species particularly suitable to study DAD. As a three-electron system, it represents the purest instance of multi-electron correlation. Simultaneous two-electron emission is the only available radiationless pathway leading to the Li^{2+} ion in its ground electronic state. Since the resonance energy is below the lowest $Li^{+}*$ threshold, no intermediate states are available for the cascade pathway. Hence, the analysis of DAD is greatly simplified and more transparent. As a few-electron system, the lithium atom is also accessible to a less approximate theoretical description, allowing for highly accurate calculations.

The one-step double autoionization of the $Li^*(2s^22p\ ^2P^0)$ resonance was first observed by Azuma *et al* [71] in a photoion yield spectra. The nonresonant double-to-single photoionization ratio was estimated in this work as $1.3 \pm 0.3\%$. Wehlitz and coworkers [72] studied the resonance in a similar but more accurate photoionization experiment in the photon energy range 141.5–143.5 eV. By analyzing the line profile of the resonance in the Li^+ and Li^{2+} photoion yield spectra, they determined the resonant double ionization BR as 3.3%.

The first theoretical study of the DAD rate of $Li^*(2s^22p\ ^2P^0)$ state was the MBPT calculation with LS-coupled intermediate states by Simons and Kelly [28]. The calculated DAD BR was 6.8%, i.e., by a factor of two larger than the experimental value. The individual shake-off and knock-out contributions were identified as 53% and 32% of the DAD rate, respectively. Remaining 15% of the intensity stem from terms of the transition amplitude that cannot be associated with either of these basic mechanisms. A slightly lower value of 5% for the DAD BR was obtained by Berrington and Nakazaki using *R*-matrix theory [73].

A very accurate nonperturbative approach for three-electron atomic systems, based on the time-dependent close-coupling method was developed by Pindzola *et al* [74]. The electrons are described by a nine-dimensional wave function with a numerical lattice representation of the radial dimensions and a coupled-channels expression for the six angular dimensions. In this way, correlation effects among the three electrons moving in the Coulomb field of the nucleus are fully taken into account. For the DAD BR of $Li^*(2s^22p\ ^2P^0)$, the method yielded the value of 3.7%, in excellent agreement with the experimental value of Wehlitz *et al* [72].

Two-electron emission can also contribute to electron-impact ionization of Li or Li-like ions in a process called resonant recombination auto double-ionization:

$$e^- + [A(1s^22s)]^{(q+1)+} \longrightarrow [A(1s\ 2s\ 2p\ nl)]^{q+,*} \longrightarrow [A(1s^2)]^{(q+2)+} + 2e^-. \quad (9)$$

MBPT calculations of the corresponding cross sections in the Li isoelectronic sequence for recombination through the $1s2s^22p\ ^3P$ intermediate states (population of the singlet term is negligible in the recombination step) was conducted by Pindzola and Griffin [31]. The lowest-order formulae (2) and (4) were used for the evaluation of single and double Auger rates of the intermediate states, with certain higher-order effects being included through the use of multiconfigurational wave functions. Specifically, for $O^{4+}(1s2s^22p\ ^3P)$ the calculations gave an upper limit for the DAD BR of 0.9%. This is consistent with the experiment of Rinn *et al* [75] who did not detect any DAD contribution to electron-impact ionization of O^{5+} but the determination was limited by a noise level of at least 1%. However, the calculations suffer from large uncertainties stemming from an unknown relative phase between the direct and exchange Coulomb matrix elements entering equation (4). Furthermore, two different single particle basis sets also yield notably diverse decay rates.

2.4. Double Auger decay in molecules

DAD in molecules poses an intrinsically even more intricate problem than in atoms. Multiply charged molecular ions resulting from AD are unstable species prone to dissociation. Nuclear dynamics not only shifts and broadens the lines in the electron spectra but the possible dissociation often leads to complex relaxation pathways, namely in the cascade processes. An example was given already in section 2.2 in neon dimer, where atomic DAD results in a dissociative two-site ionic state through radiationless charge transfer. In larger molecules, the measured spectra are typically strongly sensitive to the localization of initial inner-shell vacancies. Also, the known pace of dissociation of autoionizing states can provide a natural in-built clock to measure the electronic decay lifetimes in time-resolved experiments.

Using time-of-flight mass spectrometry and photoion-photoion coincidence techniques, Hitchcock *et al* [76] showed that carbon $1s \rightarrow 2\pi^*$ photoexcitation in CO produces a significant yield (about 32%) of doubly charged ionic fragments, indicating the occurrence of resonant DAD. Three electron emission was detected in about 2% of decay events. Detailed experimental analysis of the decay of the $C(1s \rightarrow 2\pi^*)$ resonance was afterwards conducted by Journel and coworkers [6]. They employed ion–ion–electron and electron–electron coincidence techniques to study spectra of all products of four different channels accessible via DAD: $C^+ + O^+ + 2e^-$, $(CO)^{2+} + 2e^-$, $C^{2+} + O + 2e^-$ and $C + O^{2+} + 2e^-$. Both direct and cascade DAD mechanisms have been observed, including complex sequential processes such as dissociation of the intermediate molecular ion $CO^{+}*$ followed by autoionization of the oxygen fragment. A clear signature of the direct process is provided by the nonzero intensity of electron emission in the energy region where no $(CO)^{+}*$ intermediate states are found. The lower bound for the contribution of the direct mechanism was determined as 20% of the overall DAD. For higher core-excited resonances, DAD was found to proceed almost exclusively via cascade pathways [77].

Eland and coworkers studied triple ionization in decay of core-ionized states of methane [78], OCS [79] and carbon disulfide [80] by use of three-electron coincidence

spectroscopy. In CS_2, the triple photoionization yield was found to be 12% for a photon energy just above the S(2p) edge and 24% above the S(2s) edge. For comparison, in the OCS molecule, ionization by a photon with energy just above the S(2p) edge leads to triple ionization only in 2% of the events, increasing no higher than 6% if the photon energy is above the C(1s) and O (1s) edges. In the experiments, both direct and cascade DAD have been detected, however, BR were not extracted by the authors.

The cascade processes were found to be characterized by emission of a very low energy electron, therefore, selection of coincidence events where both Auger electron energies are above certain values effectively eliminates the cascade mechanism from the collected data. It allows for a thorough analysis of the direct DAD spectrum and triply ionized final states population. Methane provides a particularly useful example for such a study because its very simple structure enables transparent identification of the orbital character of the final states. It was found that the inner-valence C(2s)-like orbital has a greater tendency to provide the Auger electrons than the outer-valence electrons. Furthermore, doublet spin states are preferentially populated compared to quartet states in the DAD from initially closed shells [79]. Analogous preference for singlet over triplet doubly ionized final states has been reported previously for single AD from closed-shell species [81, 82].

3. Triple Auger decay

In section 2.2 we mentioned the possible observation of TAD in the neon atom [46, 49]. Recent outstanding experimental advances have made it possible to detect such weak processes more reliably. In analogy to hollow lithium atoms, the $C^+(1s2s^22p^2\ ^2D,\ ^2P)$ resonances of a singly charged carbon atom represent ideal metastable states to study TAD. Indeed, for a five-electron configuration with a K vacancy and four electrons in the L-shell, the simultaneous emission of three electrons is the only radiationless mechanism available for the production of C^{4+} ions in the ground electronic state, see figure 1(C). Detection of the helium-like C^{4+} ions therefore unambiguously identifies direct TAD.

Müller *et al* [83] investigated single, double and triple ionization of C^+ by single photons in the energy range of 286–326 eV, i.e., in the region from the lowest-energy K-vacancy resonances to beyond the K ionization threshold. Clear signatures of the $C^+(1s2s^22p^2\ ^2D,\ ^2P)$ resonances were found in the triple-ionization channel. Since alternative multi-photon and collision processes leading to the production of C^{4+} ions are ruled out as extremely weak in comparison with the single-photon resonant excitation, the measurement provides clear experimental evidence for direct TAD with BR approximately 0.013%. For comparison, the DAD BRs were determined as 2.59% and 3.22% for the ^2D and ^2P terms, respectively. As the correlated dynamics of the three unbound electrons in the external field of the closed-shell $C^{4+}(1s^2)$ ion is not complicated by sequential decay, TAD in C^+ provides access to experimental study of the so-called four-body Coulomb problem previously explored in triple photoionization of Li [84].

4. Collective Auger decay

An ion with two inner valence vacancies and several electrons in the outer shells will most probably decay by two separate Auger transitions, each one filling a single vacancy. However, there is a possibility for a three-electron AD process in which the two inner-shell holes recombine simultaneously and the total relaxation energy is carried away by a third electron. In the present review, we call this process (three-electron) CAD, referring to the collective recombination of two vacancies. In existing literature, the transition is often referred to as DAD which may, however, cause confusion with the process discussed in the previous sections.

Different CAD transitions are depicted in figure 1(D). The most widely studied case (D.I) results in the ejection of electrons with about twice the normal Auger energy. It is found to be typically orders of magnitude slower than the competing two-electron transition. Consequently, the literature on CAD is much less extensive than that on DAD. Nevertheless, a number of both experimental and theoretical studies have been conducted. Furthermore, recent findings show that the extent of CAD can increase under favorable conditions. Indeed, there exist doubly inner-valence ionized states for which CAD is the only nonradiative decay process available. Particularly in molecules the CAD rate can be greatly enhanced by very strong configuration interaction in the valence and sub-valence shells, reaching values comparable with the ordinary two-electron AD. The CAD probability relative to the AD one is the most important quantity to assess the significance of this relaxation process. In the following, we use the notation $R_3 = \Gamma_{CAD}/\Gamma_{AD}$ for the ratio between the total CAD and AD rates if both processes are available for a given metastable state.

4.1. Experimental evidence for collective Auger decay in atoms

A CAD LL–MMM transition was first proposed in 1971 as an explanation for a peak corresponding to the electron energy $E_e = 500$ eV, observed by Ogurtsov *et al* [85] in the spectrum of electrons produced in $Ar^+ - Ar$ collisions. However, the spectral feature itself was later questioned as an apparatus effect by Rudd and coworkers [86], who observed no such signal in similar measurements.

More convincing experiment was performed in 1975 by Afrosimov *et al* [11], who studied the decay of two $L_{2,3}$ vacancies produced in collisions of N^+, N_2^+, Ar^+ and Cl^+ ions with Ar atoms. In these collisions, the two vacancies are created in Ar, with the exception of collisions with Cl^+ where the $L_{2,3}$ holes are produced with high probability in the Cl atom. In both cases, sequential decay by two ordinary L–MM Auger transitions is found to be almost completely dominant. The observed relative probability of the LL–MMM CAD transition lies in the range 10^{-3}–10^{-4}. Very recently, well-resolved CAD spectrum in Ar was measured by Žitnik

et al [87]. The LL vacancy states were prepared by a single-photon K-shell ionization and subsequent K–LL decay. For the LL($^1D_2$) double vacancy state, the R_3 ratio was determined as 2.2×10^{-3}. Furthermore, comparison of linewidths of the L–MM Auger and LL–MMM CAD signals showed that the double L-vacancy state decays more than two times faster compared to a single L-vacancy, similarly to double K-vacancy states [88, 89]. From the full width at half maximum of the Lorentzian component in the Voigt profile fitted to the CAD spectral line, the decay rate of the LL($^1D_2$) double vacancy state can be estimated as 5×10^{14} s^{-1}, giving the CAD rate of the order of 10^{12} s^{-1}.

KK–LLL CAD of double core hole states in C and N was observed in ion-atom collisions by Afrosimov *et al* [90]. The measurement yielded comparable relative CAD intensities, namely 2.2×10^{-4} for C and 3.1×10^{-4} for N. The KK–LLL CAD in nitrogen was also observed by Moretto-Capelle and coworkers [1] as weak features between 570 and 950 eV in the electron spectrum from slow bare N^{7+} ions approaching a Si surface. In a similar experiment, Folkerts *et al* [2] studied electron spectra arising from collisions of C^{6+} and N^{7+} ions on a Ni surface, also detecting distinct peaks at about twice the ordinary Auger energy (i.e., around 592 eV). In this type of experiment, the bare ions already possess the required inner-shell holes and outer electrons are captured from the metal surface. The capture process is very efficient and many electrons are attached into the L-shell before the inner holes can decay. Rapid capture is vital for potential observation of CAD since at least three electrons in the L-shell are necessary for the collective decay to be possible. The measured spectra made it possible to determine the R_3 ratio as $(3.4 \pm 0.6) \times 10^{-4}$ for carbon and $(3.1 \pm 0.4) \times 10^{-4}$ for nitrogen [2]. Comparing to the very similar CAD probabilities measured by Afrosimov *et al* [90] given above, these numbers suggest a complete filling of the L-shell in bare ion–surface collisions prior to the recombination of the core holes. This conclusion is further supported by the energy positions of the corresponding peaks in the electron spectra, which indicate large shielding of the core charge by the L spectator electrons.

Another way to prepare ions with electronic configurations allowing KK–LLL transitions is beam-foil excitation, where a swift ion beam interacts with a thin foil. In contrast to the slow ion–surface collision experiments, Auger electrons from the target foil cannot obscure the spectra since Auger electron emission from the fast projectile takes place with energies in the laboratory frame well above 10 keV. Electron emission from collisions of C^{3+} ions with carbon foils of various thickness was studied by De Filippo *et al* [13] using a time-of-flight technique. A weak structure is visible in the collected spectra at the flight time corresponding to an energy of (647 ± 110) eV in the projectile reference frame. Even though the energy position is displaced compared to the value of 592 eV given by Folkerts *et al* [2], the results are compatible within the experimental error margins and the KK–LLL CAD is the only conceivable explanation for the observed electrons. The R_3 ratio could not be determined since the normal Auger peak is not visible for kinematic reasons.

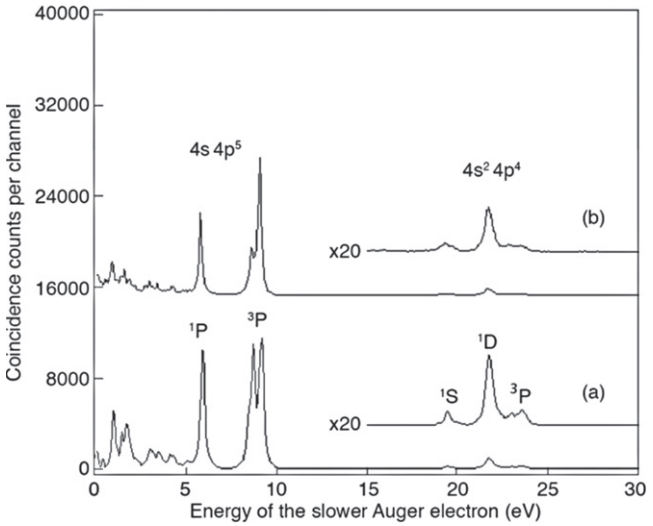

Figure 6. Spectra of the second Auger electron in Kr resonant Auger decay: (a) at 91.2 eV photon energy, after detection of a first Auger electron within the 29.1 eV line corresponding to the population of the $Kr^+(3d^{10}4s^04p^65p)$ resonance, and (b) at 92.4 eV photon energy after detection of a first electron in the similar line at 30.8 eV. Reproduced with permission from [91].

Lee *et al* [12] demonstrated, with the Kr atom as an example, that collective decay is also a possible relaxation pathway for a final state of a spectator resonant Auger transition:

$$Kr^*(3d^94s^24p^65p) \longrightarrow Kr^+(3d^{10}4s^04p^65p) + e_A^- \longrightarrow Kr^{2+}(3d^{10}4s^24p^4) + e_{CAD}^-. \quad (10)$$

The identification of the observed lines in the measured electron spectra as CAD is not unique and hinges on the correct assignment of the intermediate state of the decay cascade. Other processes emitting electrons with similar energies cannot be completely ruled out. The alternative pathways, however, require rather complicated intermediate states to be formed and appear to be even less probable. According to the authors, the interpretation could ideally be corroborated by a coincidence measurement.

Such an experiment was carried out recently by Eland *et al* [91] and indeed confirmed the three-electron character of the second step of the decay cascade initiated by 3d → 5p excitation of Kr. The experiment combined energy-selected synchrotron light with a magnetic bottle time-of-flight spectrometer, which enabled the detection of the photoelectron, the resonant Auger electron and the CAD electron in coincidence. The 29.3 eV resonant Auger electron unambiguously selects events in which the intermediate $Kr^+(3d^{10}4s^04p^65p)$ double-vacancy state is populated. The resulting triple ionization spectrum clearly contains a group of lines corresponding to formation of Kr^{2+} in its ground state configuration $3d^{10}4s^24p^4$, see figure 6. At lower electron energies, the more intense lines correspond to formation of excited $Kr^{2+}(3d^{10}4s^14p^5)$ ions that are accessible by competing two-electron transitions. The uncommonly high R_3 ratio of about 2.5% is connected with the low energy of 20–25 eV of the outgoing CAD electron. Analysis of the

$Kr^{+}(3d^{10}4s^{0}4p^{6}5p)$ wavefunction calculated using the extended second order algebraic diagrammatic construction [92] suggests that the decay rate is also significantly enhanced by the very efficient configuration mixing in the Kr valence shell, but detailed theoretical analysis of CAD in Kr is not yet available.

Information on the CAD rate can also be obtained from the study of trielectronic recombination. In this process, attachment of a single electron to an ion is accompanied by simultaneous excitation of two core electrons. Therefore, trielectronic recombination can be viewed as a time-reversal process to CAD. As such, its rate is connected to the CAD rate through the principle of detailed balance. Trielectronic recombination to He-like Kr^{34+} ions was studied by Chevallier *et al* [16] by using the method of channeling the ions through a thin Si crystal. Since the KK–LLL resonant trielectronic capture is followed by stabilization involving the emission of two K photons, the trielectronic recombination signal can be unambiguously extracted from a K x-ray–K x-ray–Kr^{33+} triple coincidence measurement. The upper limit for the trielectronic recombination cross section was determined as $1.9 \times 10^{-27}\mathrm{cm}^2$. This corresponds to the ratio of tri- to dielectronic recombination cross sections of 5×10^{-6}, which is directly comparable with the relative intensity of CAD from the double core hole state of the Li-like krypton. To our knowledge, there is no direct observation of CAD in high-Z atoms, which could be compared to this result. However, considering that the experimental value represents an upper limit, it is in reasonable agreement with the R_3 ratio of 2.8×10^{-7}, calculated by Marques and coworkers [14]. These results indicate that in high-Z atoms the significance of CAD drops significantly by about two orders of magnitude. The explanation given by Vaeck and Hansen [15], which is based on the decrease of the efficiency of shake-down mechanism, is discussed in the following subsection.

4.2. Theory of collective Auger decay

Two early theoretical studies of CAD rates were carried out by Ivanov *et al* [93] and by Simons and Kelly [94]. Ivanov and coworkers calculated CAD rates for Li-like ions with different atomic numbers Z in second order of MBPT, employing Coulomb single-electron wave functions as basis. For the electronic configuration $2s^22p$, a simple dependence of the CAD rate on the atomic number Z was derived, namely

$$\Gamma_{\mathrm{CAD}} = 0.126 \times 10^{13} Z^{-2}\ \mathrm{s}^{-1}. \tag{11}$$

Specifically, for the Li atom equation (11) yields a rate of $1.4 \times 10^{11}\,\mathrm{s}^{-1}$. The calculated single AD rate is $2.0 \times 10^{14}\,\mathrm{s}^{-1}$ [94], which gives the R_3 ratio of 7×10^{-4}, in accordance with the available experimental results for low-Z atoms. Using an approximate dependence of the AD and CAD decay rates on the number of electrons available for the decay transitions, the result can be extrapolated to atoms with more than three electrons. For double K-vacancy states of C and N, Ivanov *et al* [93] estimated the R_3 ratios as 2.1×10^{-4} and 2.3×10^{-4}, respectively. These values are in very good agreement with the experimental results 2.2×10^{-4} for C and 3.1×10^{-4} for N [90]. From the decomposition of the transition amplitude it follows that the contributions to the CAD process stemming from correlation in the initial and final states of the process are equally important. This finding is interesting in comparison with two-electron–one-photon transitions where the probability is almost completely determined by a first-order correction to the final state wave function [93, 95].

Single and CAD rates of the $2s^22p$ excited state of lithium were also calculated by Simons and Kelly [94] at the same order of MBPT but with LS-coupled intermediate states and a HF single-electron basis. The calculated CAD rate is $1.57 \times 10^{11}\,\mathrm{s}^{-1}$ ($R_3 = 8 \times 10^{-4}$). The 10% disagreement with the calculation of Ivanov *et al* [93] is explained by inclusion of $2p^3$ mixing in the initial state. For direct comparison, Simons and Kelly evaluated also the radiative decay rate for the excited state of interest, obtaining a value 6.44 times smaller than the CAD rate. It shows that even higher-order multi-electron processes are still more efficient than interaction with the electromagnetic field.

A comprehensive MBPT study of correlated decay of two vacancies in Ne, Ar and Kr atoms was performed by Amusia and Lee [9]. Contrary to previous studies, which considered only transitions where the initial holes belong to the inner shells and final vacancies to outer shells (transition of type D.I in figure 1), Amusia and Lee considered also transitions of types D.II and D.III with one final vacancy belonging to a deeper shell (with respect to the initial hole). The energy gained from the recombination of one of the initial vacancies is, therefore, distributed among two electrons to excite one and ionize another. Such transitions lead to the emission of slower electrons compared to the decay of type D.I.

For CAD of type D.I in $Ne^{2+}(1s^{-2})$ and $Ar^{2+}(2s^{-2})$, Amusia and Lee obtained total decay rates of $2.57 \times 10^{11}\,\mathrm{s}^{-1}$ and $8.34 \times 10^{11}\,\mathrm{s}^{-1}$, respectively. In Ne, the analysis of the MBPT contributions to the total transition amplitude shows that it is dominated by the imaginary part, which is proportional to the products of the Coulomb matrix elements

$$\mathrm{Im}\, A \sim \langle \mathrm{i}_1 k_0 | V | \mathrm{f}_1 \mathrm{f}_2 \rangle \langle \mathrm{i}_2 q | V | k_0\, \mathrm{f}_3 \rangle. \tag{12}$$

where the spin orbitals i_α and f_β correspond to the initial and final vacancies, respectively, q to the emitted CAD electron and k_0 to a virtual electron with an energy equivalent to that of an ordinary $\mathrm{i}_1 \rightarrow \mathrm{f}_1\mathrm{f}_2$ Auger transition. We have employed the notation for Coulomb integrals over spin orbitals

$$\langle ik|V|jl\rangle = \int \psi_i^*(\mathbf{r}_1)\psi_k^*(\mathbf{r}_2)\frac{1}{|\mathbf{r}_1 - \mathbf{r}_2|}\psi_j(\mathbf{r}_1)\psi_l(\mathbf{r}_2)\mathrm{d}\mathbf{r}_1\mathrm{d}\mathbf{r}_2. \tag{13}$$

The CAD transition amplitude (12) leads to a two-step interpretation of the process. First, ordinary AD of one 1s hole takes place emitting an electron k_0. This electron then recombines with the second 1s vacancy, leading to emission of the CAD electron q. In the heavier Ar atom, such a dominance of the imaginary parts of the MBPT transition amplitudes is found only for one particular transition, namely $2s^{-2} \rightarrow 3s^{-2}3p^{-1} + q$, but the corresponding partial decay

rate is one order of magnitude larger than for other channels and this pathway again dominates the collective decay.

Transitions of type D.II and D.III were studied in suitable metastable states of doubly ionized Ar and Kr. The measurement of CAD after resonant AD in Kr [91] discussed in a previous section indicates that a lower energy of the emitted electron can lead to a significant increase in the efficiency of the collective decay. This result is in full accordance with the calculations. For instance, the $3s^{-1}4p^{-1} \rightarrow 3d^{-1}4s^{-2}$ transitions of type D.III in Kr have decay rates around 10^{13} s^{-1}, i.e., two orders of magnitude larger than the typical values obtained for type D.I decay pathways [9]. The CAD electron is in this case emitted with an energy of about 105 eV, compared to about 582 eV for the dominant CAD transition of type D.I in Ar $^{2+}(2s^{-2})$.

Valuable insight into the mechanism of CAD is provided by the theoretical papers of Vaeck and Hansen [15] and of Marques *et al* [14] who studied CAD in low-Z and high-Z atoms respectively. In double K-hole states of low-Z atoms, the main contribution to the CAD process stems from the $2s \rightarrow 1s$ shake-down mechanism accompanying normal K–LL Auger transition. If shake-down dominates, the ratio between the particular CAD transition probability and the probability of the corresponding normal AD channel can be estimated solely from the overlap integral between the initial state 2s and final state 1s orbitals as [15]

$$\Gamma_p^{\mathrm{CAD}} / \Gamma_p^{\mathrm{AD}} \approx q\, |\langle 1s_f | 2s_i \rangle|^2 . \qquad (14)$$

The factor q equals two if there is one 2s electron in the final state of the normal AD and $q = 1$ otherwise. An example of the former case is the CAD transition $2s2p^N \rightarrow 1s^2 2p^{N-2}$, which corresponds to $2s2p^N \rightarrow 1s2s2p^{N-2}$ AD channel with shake-down of the 2s electron. For the $2s^2 2p^6 \rightarrow 1s^2 2p^5 + e^-_{\mathrm{CAD}}$ transition in $Ne^{2+}(1s^{-2})$, the shake-down approximation (14) gives a partial rate 1.5×10^{11} s^{-1}, in excellent agreement with the full calculation by Amusia and Lee [9], who obtained 1.6×10^{11} s^{-1} for this partial rate.

If the shake-down mechanism is operative, typical values for the CAD rate are of the order of 10^{11} s^{-1}, corresponding to R_3 ratios of 10^{-4}. Purely correlation-driven transitions (i.e., those involving only 2p electrons) lead to relative CAD probabilities which are about two orders of magnitude smaller. For example, for the $N^{(2-M)+}(2s^M 2p^5)$ double core hole state of the nitrogen atom, the R_3 ratio was calculated as 4.4×10^{-4} and 1.7×10^{-4} for initial configurations with two and one 2s electrons, respectively. For the initially empty 2s orbital ($M = 0$) the R_3 ratio drops down to 3.0×10^{-6} [15]. Comparison with the R_3 ratio of $(3.1 \pm 0.4) \times 10^{-4}$ measured in bare ion–surface collisions by Folkerts *et al* [2] indicates that at least one 2s electron is captured prior to the decay event.

Marques *et al* [14] focused on high-Z atoms and calculated the AD and CAD rates for lithium-like Kr, Nb and Gd ions with all three electrons in the L-shell. The rates were computed using multiconfigurational Dirac–Fock bound-state wave functions. The shake-off mechanism was not included, but since with increasing atomic number the $\langle 1s_f | 2s_i \rangle$ overlap decreases the approach is justified. Indeed, for the two-electron–one-photon radiative transition, the effects of relaxation were estimated to account for about 20% and only 8% of the total intensity for $Z = 36$ and $Z = 54$, respectively [14]. Similar trends can be expected also in radiationless transitions. Therefore, in higher-Z atoms the collective decay is indeed a purely correlation-driven process with characteristic decay rates of order 10^8 s^{-1} and relative intensities $R_3 \approx 10^{-7}$.

From the above results it follows that for atomic ions the measured and calculated CAD rates agree at least semi-quantitatively in all studied cases. If the CAD is purely correlation-driven, it proceeds on a nanosecond time scale and its relative probability with respect to competing two-electron transitions is extremely low. This makes a direct observation of the process immensely difficult. In lighter atoms, however, the efficiency of the CAD of double core hole states can be significantly enhanced by the shake-down mechanism. Resulting CAD probabilities are close to 0.1% and the process becomes accessible to experiment. The CAD rate increases also if the energy of the emitted electron is low. This is exemplified by the decay cascade from resonantly excited Kr [12, 91], in which the CAD electron emitted in the second step carries energy only about 20–25 eV.

5. Collective decay in molecules

In previous section we have seen that in the case of atomic double core holes the rates of collective decay processes lie in the range 10^8 s^{-1} – 10^{11} s^{-1} and the probabilities relative to ordinary AD are of the order of 10^{-4}–10^{-7}. Therefore, CAD does not play a significant role in the relaxation of such highly excited states. It has been shown recently [18] that the situation can be radically different for doubly inner-valence ionized states of a variety of molecular species. Not only is CAD often the single possible radiationless decay channel for this class of metastable states, but its rate can reach values of the order 10^{14} s^{-1}, i.e. it can proceed on the few-femtosecond time scale reminiscent of normal Auger transitions.

Doubly inner-valence ionized molecular states, however, often present an assignment problem due to the so-called molecular orbital picture breakdown [96]. Because of the very efficient configuration mixing in the valence shell, doubly inner-valence ionized states often cannot be assigned to any single two-hole (2h) configuration corresponding to the removal of electrons from two specific molecular spin-orbitals. This situation is typical for states related to ionization from shallow inner-valence orbitals, such as carbon or nitrogen 2s orbitals. Consequently, relaxation of such states cannot be reliably interpreted as collective decay.

To avoid these problems, Feifel *et al* [18] focused in their joint experimental and theoretical study of CAD on small molecules bearing relatively deep (e.g., F $2s^{-2}$) double inner-valence holes. Using the *ab initio* Fano-ADC method [97] they calculated CAD rates for a few such double vacancy states in small molecular species. The results range from

$7.7 \times 10^{13}\,s^{-1}$ for the F_2 molecule up to $9.1 \times 10^{14}\,s^{-1}$ for the double O 2s hole in the OH^- molecular anion. One reason for these extraordinary high rates is the low energy (0–20 eV) of the secondary electrons emitted in the CAD process. This, however, cannot fully account for the ultrafast character of the three-electron transitions.

The second and more important reason can be traced to the aforementioned efficient configuration interaction both in the initial doubly ionized and final triply outer-valence ionized states of the decay. In the frozen-orbital single-configuration picture the CAD process is forbidden, i.e. the main 2h configuration representing the initial state is not coupled directly to the final states characterized by three holes and an electron in the continuum. However, even a modest configuration mixing can change the situation dramatically and make the transition partially allowed. The numerical calculations show (see table I in [18]) that for the studied doubly inner-valence ionized states, shake-up type configurations constitute up to 30%–40% of the associated wavefunctions. Some of those configurations are coupled directly to the main configurations of the CAD final states. At the other extreme, in the expansion of the final states the dominant configurations with three outer-valence holes are mixed with configurations possessing one inner-valence hole, again contributing to direct coupling of the correlated initial and final states.

To confirm the theoretical results, coincidence experiments were carried out on the CH_3F molecule [18]. The experimental setup was similar to that used to study CAD in Kr atom [91], i.e. energy-selected synchrotron light from the storage ring BESSY II was combined with a magnetic bottle time-of-flight electron spectrometer. Collective decay was observed in Auger-CAD cascades initiated by C or F core ionization. The double F 2s inner-valence vacancy state of CH_3F^{2+} was located in both the carbon and fluorine Auger spectra around 98 eV ionization energy. The experimental setup made it possible to detect in coincidence all three electrons produced in the photoionization-induced cascade, i.e. the core photoelectron and two secondary electrons. By choosing triple coincidence events where one electron signals the initial 1s hole formation, a second electron shows population of the 98 eV $CH_3F(2s^{-2})$ state and a third electron confirms its subsequent electronic decay, triple-ionization spectra produced through the intermediate formation of the desired double inner-valence hole state were extracted. The spectra are shown as error bars in figure 7 together with theoretical simulations. The fact that they do not extend to ionization energies below 70 eV and have a peak near 90 eV suggests that the CAD process populating the triply ionized states from the intermediate F 2s double hole state is very rapid. If it did not occur on a roughly femtosecond time scale, Coulomb explosion of the molecular ion would precede it and the separated fragments would show as intensity in the spectra at lower energy.

This conclusion is supported by the theoretical simulations shown in figure 7 as solid curves. In the calculations, nuclear dynamics along the essential C–F bond in the intermediate $CH_3F^{2+}(2s^{-2})$ state were taken into account, assuming this state is populated instantaneously by normal AD at $R_{(C-F)} = 1.315$ Å for the C(1s) cascade and at $R_{(C-F)} = 1.4$ Å for the F(1s) cascade. For more details, see [18]. Since only three-electron relaxation transitions were considered in the evaluation of the decay width of the $CH_3F^{2+}(2s^{-2})$ intermediate state, the excellent agreement between the simulations (blue curves in figure 7) and experiment confirms that the decay of the double F 2s hole state is dominated by ultrafast CAD. To further verify the sensitivity of the spectra to the decay rates, simulations were also performed with the *ab initio* decay widths scaled down by a factor of 5 (magenta lines in figure 7). Slower decay obviously leads to notably poorer agreement with the experimental spectra, particularly in the case of the C 1s Auger route.

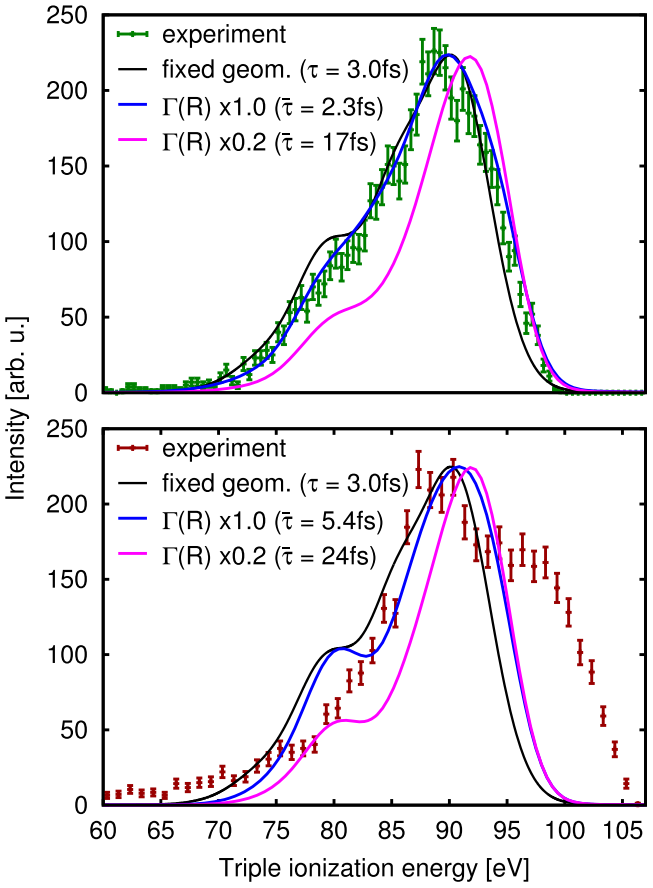

Figure 7. Experimental triple ionization spectra acquired from the carbon core (upper panel, green error bars) and from the fluorine core ionization initiated cascade (lower panel, red error bars). The black curves show the theoretical spectra calculated at fixed equilibrium geometry of the molecule. The blue curves reflect spectra obtained with the inclusion of nuclear motion along the C–F bond in the intermediate $CH_3F^{2+}(2s^{-2})$ state, assuming this state is populated by the Auger decay at $R_{(C-F)} = 1.315$ Å for the C(1s) cascade and at $R_{(C-F)} = 1.4$ Å for the F(1s) cascade. The magenta spectra are calculated in the same way but with the *ab initio* CAD width scaled down by a factor of 5. In all theoretical spectra, only the decay channels accessible exclusively by the three-electron transitions were taken into account. Reproduced with permission from [18], Copyright 2016 American Physical Society.

6. Collective interatomic Coulombic decay in clusters

Over the last two decades, considerable attention has been paid to different interatomic decay processes in van der Waals or hydrogen-bonded clusters. A model example is the ICD predicted theoretically by Cederbaum *et al* [4]. In ICD an inner-shell vacancy on one cluster subunit (atom or molecule) recombines with an outer-shell electron and the excess energy is utilized to ionize neighboring species, see figure 2(A). This process is characteristic of inner-valence vacancies such as $Ne(2s^{-1})$, which are not energetic enough to undergo AD in an isolated atom. The ICD process in a cluster is still energetically allowed due to the existence of final doubly ionized states with positive charges residing on different and separated cluster subunits, reducing the Coulomb repulsion. Depending on the size and composition of the cluster, ICD occurs on time scales from hundreds of femtoseconds [98–100] down to several femtoseconds [101–104]. The rate of interatomic relaxation transitions transitions can be also strongly influenced by the nuclear dynamics induced by ionization or excitation of the system [105–107]. Recently, the importance of interatomic decay processes was highlighted through its possible consequences for radiation biology [108, 109]. ICD was shown to be relevant also in quantum dots [110–112]. For up-to-date review on ICD and related processes see [21].

Contrary to the Auger process, which is mediated by electronic correlation *within an atom or molecule*, ICD and related interatomic phenomena are driven by electronic correlation *between two or even more atoms*. In the context of the present review it is natural to ask whether there exist also multi-electron processes similar to double or collective Auger transitions, mediated by such nonlocal correlation. Averbukh and Kolorenč [22] proposed collective ICD of multiple vacancies in clusters, analogous to CAD, in which two inner-valence vacancies in a multiply ionized cluster decay simultaneously, emitting a single electron from a neighboring atom. For example, in mixed Kr–Ar clusters the process can occur following 4s ionization of two neighboring Kr atoms as shown in figure 2(B). In analogy to the established physical picture of ICD as a virtual photon transition [102, 113], this process can be interpreted using a multi-virtual photon mechanism.

Due to the very low Kr 4p → 4s relaxation energy, a single Kr 4s vacancy cannot decay by an Auger or ICD process and collective ICD represents the only radiationless decay channel. Similar conditions in which collective ICD occurs without competition of two-electron relaxation transitions can arise in a wide variety of multiply inner-valence ionized clusters. Examples can be found among clusters of nonmetal hydrides (HCl, HBr, H_2S, PH_3,...) or small hydrocarbon molecules. Despite being the only radiationless decay mode, however, collective ICD can be quenched by dissociative nuclear dynamics of the multiply ionized cluster. In order to assess the feasibility of this higher-order process, Averbukh and Kolorenč [22] studied the competition between electronic decay and cluster disintegration in the specific example of a Kr_2Ar trimer using the Fano-ADC method [97] for the decay widths and simulation of the wave packet evolution on complex potentials. At the equilibrium geometry, the calculated collective decay rate is $3 \times 10^{12} s^{-1}$. The corresponding lifetime of about 300 fs is five orders of magnitude shorter than that of the radiative decay [114] but is comparable to the characteristic times associated with nuclear dynamics. Therefore, the latter has to be taken into account for proper evaluation of the importance of the electronic transition being considered. The calculated collective ICD yields range from 30% to 65%, depending on the mechanism of the initial double ionization. Hence, collective decay can contribute substantially to the accumulation and redistribution of positive charges in a cluster exposed to ionizing radiation. Furthermore, collective ICD is expected to be even more significant if the cluster is initially multiply excited rather than ionized since under such conditions the multi-electronic process proceeds without the competition from cluster disintegration [23].

A similar collective ICD transition of two inner-valence vacancies localized on a single atom is possible in Ne_2 following single-site double Ne 2s ionization [115] and in NeAr dimers after double Ar 3s ionization [116]. The three-electron decay

$$\begin{aligned} NeAr^{2+}(3s^{-2}\ {}^1S) \longrightarrow Ne^{+}(2p^{-1}\ {}^2P) \\ + Ar^{+}(3p^{-2}\ {}^3P) + e^{-}_{ICD} \end{aligned} \quad (15)$$

was indeed observed by Ouchi *et al* [24] by means of momentum-resolved electron–ion multi-coincidence spectroscopy. The results suggest that the collective ICD is significantly faster than other available relaxation processes like radiative decay or charge transfer. It is interesting to note that for the particular transition represented in equation (15), the usually dominant energy transfer mechanism is effectively forbidden due to the different spin multiplicity of the initial and final two-vacancy states of Ar. Therefore, electron exchange is required between the Ne and Ar atoms. Such transitions are governed by the overlap between the participating orbitals residing on the neighboring atoms and the associated decay rates decrease exponentially with increasing interatomic distance. Consequently the decay takes place dominantly at the smallest possible bond length.

Despite the scarcity of work on multi-electron interatomic decay processes available, the results presented hitherto suggest that under certain conditions such processes can become significant or even dominant relaxation channels. This observation highlights the importance of multi-particle correlation between electrons localized on different constituents even in weakly bound aggregates. Furthermore, since the collective ICD discussed in [22] is expected to occur unhindered by other electronic processes in clusters of small hydrocarbons, it can be relevant for the mechanism of radiation damage in organic compounds. Therefore, collective processes have to be taken into account in future studies on interatomic energy and charge transfer processes.

7. Collective autoionization of nanoscale systems

When multiple photons are absorbed in a complex system upon irradiation by a powerful free electron laser, a plasma-like state can be formed where many atoms are ionized on a femtosecond time scale. With sufficiently intense fields, the formation of the so-called nanoplasma is found to be nearly independent of the type of the radiation. It can be produced by infrared radiation due to a strong resonant coupling of the cluster to the light's electric field or by ultraviolet radiation via single and multi-photon ionization. Nanoplasma can be formed also by x-ray radiation since a highly charged cluster can trap even fast photoelectrons in the keV range [117, 118]. Subsequent quick thermalization is accompanied by evaporation of slow electrons [119].

For radiation at energies below the ionization threshold photon absorption can be resonantly enhanced. The system then becomes electronically excited prior to plasma formation, which is followed by a variety of relaxation processes in which multiple electrons can participate. Recently, such decay processes named CAI were studied in He nanodroplets [25, 26]. For photon energies below the ionization threshold, multiple photons are required to ionize the system. The ionization can proceed either via multiphoton absorption of a single atom or via absorption of single photons by multiple atoms followed by CAI. The basic mechanism underlying CAI is equivalent to two-electron ICD between two excited atoms as proposed by Kuleff *et al* [23], however, a number of alternative pathways involving three or more electrons may be operative [26]. Experimentally, CAI can be distinguished from multiphoton ionization by utilizing the first-order perturbation theory formula for the ionization rate

$$\Gamma = \sigma I^n, \tag{16}$$

where σ is the ionization cross section, I is the radiation intensity and n the number of absorbed photons [25]. Therefore, while two-photon ionization of a single atom is characterized by quadratic power dependence, in the case of CAI linear intensity dependence of the ionization rate can be expected.

LaForge *et al* [25] studied photoionization of helium nanodroplets at the FERMI FEL at three different photon energies. The measured FEL intensity dependence of the ion yield is shown in figure 8. The red circles correspond to a photon energy of 42.8 eV, well above the ionization threshold. The fitted slope of 1.07 ± 0.01 clearly shows that one-photon ionization dominates. At the nonresonant below-threshold energy of 20.0 eV (blue circles), the slope of 2.06 ± 0.09 confirms the direct two-photon ionization mechanism. The photon energy of 21.4 eV (black circles) corresponds to the $1s^2 \rightarrow 1s2p$ resonant transition in the helium cluster. At this energy the slope of the ion yield dependence on the radiation intensity is found to be 0.63 ± 0.01, which suggest that the system is indeed ionized via a CAI process. The value smaller than one is attributed to partial saturation of the $1s^2 \rightarrow 1s2p$ transition. It is a rather remarkable observation that the resonant ion yield is almost

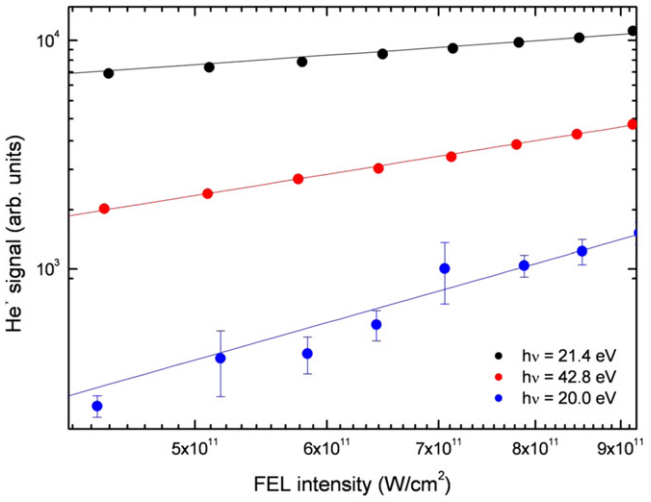

Figure 8. Logarithmic plot of the power dependence and relative ion abundances from helium nanodroplets at the photon energies of 21.4 eV (black circles), 42.8 eV (red circles) and 20.0 eV (blue circles) along with power dependence fits (lines of corresponding color). Reproduced with permission from [25]. Licensed under a Creative Commons Attribution 3.0 Unported license.

an order of magnitude larger than that from the direct one-photon ionization process. Note that the energy deposited into the system by two 21.4 eV photons is the same as by one 42.8 eV photon. The enhanced CAI efficiency can be explained by the large cross section of 25 Mbarn [120] of the resonant transition. For comparison, the cross section for direct ionization at 42.8 eV is 2.9 Mbarn [121].

More detailed analysis of the recorded electron spectra shows that two-electron ICD between two excited atoms is in fact suppressed in the nanoplasma state of the helium droplet and the CAI is driven by mechanisms involving three or more atoms [26], see figure 2(C). The dominant pathways can be depicted as direct two-electron emission mediated by energy exchange between three atoms (figure 2(C.I)), or as a two-step process in which ICD is followed by inelastic scattering of the emitted electron on another atom, leading to its excitation (figure 2(C.II)) or ionization (figure 2(C.III)). Both these processes are expected to give rise to broad continuous electron spectra, which are indeed observed. In contrast, the photoline due to the two-electron ICD process disappears in the spectrum recorded at the resonant energy of 21.4 eV. The suppression of the two-electron ICD provides evidence for the high efficiency of multielectron relaxation processes in a multiply excited system. Under the given experimental conditions, 50% of the atoms are expected to be excited within 20 fs, therefore, isolated doubly excited dimers are present only in the first few femtoseconds of the laser pulse. Since the estimated ICD lifetime of a doubly excited helium dimer is in the ps range, the process is quenched before it has time to take place. CAI becomes the dominant relaxation mechanism and may lead to an ion production rate much larger than that of direct ionization. CAI is expected to be of quite general character, important for many systems other than the helium clusters.

8. Summary

We have presented a detailed overview of experimental and theoretical work on selected multi-electron relaxation processes in systems of diverse complexity, going from light atoms through molecules to nanoscale clusters. These rare processes are of fundamental interest for the study of correlation in bound systems. Indeed, throughout this review we have demonstrated that simple approximations such as the different shake-off models typically fail to describe the decay transitions adequately, which demonstrates the essential role of electronic correlation as a driving force of these phenomena.

The basic measure that makes it possible to assess the level of correlation in a system quantitatively is the relative probability of multi-electron processes as compared to their ordinary two-electron variants. For the double Auger process, the characteristic probability lies in the range of a few percent in all types of environments if we restrict ourselves to the simultaneous two-electron emission. Sequential decay often leads to BRs over 30% but individual transitions of the cascade are driven by correlation between two electrons only.

The probabilities of CAD of multiple vacancies cover a much wider range. In the case of atomic double core hole states the three-electron transitions take place on a nanosecond time scale with relative probabilities as low as 10^{-7}, which made them for a long time somewhat elusive phenomena. Recently, focused searches and modern experimental techniques have led to unambiguous identification of collective decay in several systems where it either represents the only available nonradiative relaxation process or its rate is greatly enhanced. The most remarkable example is the collective decay of double inner-valence vacancy states in small molecules that can proceed on a femtosecond time scale, comparable to the ordinary AD. Besides efficient correlation in the molecular valence shells, another factor contributing to the high efficiency is the low energy of the emitted electron. This is demonstrated also in the collective decay of doubly 4s ionized krypton with a probability close to 3%.

In multiply excited or ionized clusters, too, interatomic multi-electron decay phenomena have been shown to play a significant role. If the level of excitation is sufficiently high, CAI processes can even quench the ordinary two-electron decay modes. Despite the fact that the investigation of interatomic multi-electron processes is still in its early days, it is apparent that they should be taken into account in future studies of the interaction of ionizing radiation with atomic or molecular clusters.

Acknowledgments

This work has been financially supported by the Czech Science Foundation (Project GAČR P208/12/0521), the Engineering and Physical Sciences Research Council (EPSRC, United Kingdom) through the Career Acceleration Fellowship (award EP/H003657/1) and the Programme Grant on Attosecond Dynamics (award EP/I032517/1), as well as by the Swedish Research Council (VR) and the Knut and Alice Wallenberg Foundation, Sweden.

References

[1] Moretto-Capelle P, Bordenave-Montesquieu A, Benoit-Cattin P, Andriamonje S and Andr H 1991 *Z. Phys.* D **21** S347–8
[2] Folkerts L, Das J, Bergsma S and Morgenstern R 1992 *Phys. Lett.* A **163** 73–6
[3] Young L *et al* 2010 *Nature* **466** 56–U66
[4] Cederbaum L S, Zobeley J and Tarantelli F 1997 *Phys. Rev. Lett.* **79** 4778–81
[5] Carlson T A and Krause M O 1965 *Phys. Rev. Lett.* **14** 390–2
[6] Journel L *et al* 2008 *Phys. Rev.* A **77** 042710
[7] Zeng J, Liu P, Xiang W and Yuan J 2013 *Phys. Rev.* A **87** 033419
[8] Wölfli W, Stoller C, Bonani G, Suter M and Stöckli M 1975 *Phys. Rev. Lett.* **35** 656–9
[9] Amusia M Y and Lee I S 1991 *J. Phys. B: At. Mol. Opt. Phys.* **24** 2617
[10] Hoszowska J, Dousse J C, Szlachetko J, Kayser Y, Cao W, Jagodziński P, Kavčič M and Nowak S H 2011 *Phys. Rev. Lett.* **107** 053001
[11] Afrosimov V V, Gordeev Y S, Zinovev A N, Rasulov D K and Shergin A P 1975 *JETP Lett.* **21** 249–51
[12] Lee I, Wehlitz R, Becker U and Amusia M Y 1993 *J. Phys. B: At. Mol. Opt. Phys.* **26** L41
[13] De Filippo E, Lanzanò G, Rothard H and Volant C 2008 *Phys. Rev. Lett.* **100** 233202
[14] Marques J P, Parente F, Indelicato P and Desclaux J P 1998 *J. Phys. B: At. Mol. Opt. Phys.* **31** 2897
[15] Vaeck N and Hansen J E 1992 *J. Phys. B: At. Mol. Opt. Phys.* **25** 3613
[16] Chevallier M *et al* 2000 *Phys. Rev.* A **61** 022724
[17] Schnell M *et al* 2003 *Phys. Rev. Lett.* **91** 043001
[18] Feifel R, Eland J H D, Squibb R J, Mucke M, Zagorodskikh S, Linusson P, Tarantelli F, Kolorenč P and Averbukh V 2016 *Phys. Rev. Lett.* **116** 073001
[19] Hergenhahn U 2011 *J. Electron Spectrosc. Relat. Phenom.* **184** 78–90
[20] Averbukh V *et al* 2011 *J. Electron Spectrosc. Relat. Phenom.* **183** 36–47
[21] Jahnke T 2015 *J. Phys. B: At. Mol. Opt. Phys.* **48** 082001
[22] Averbukh V and Kolorenč P 2009 *Phys. Rev. Lett.* **103** 183001
[23] Kuleff A I, Gokhberg K, Kopelke S and Cederbaum L S 2010 *Phys. Rev. Lett.* **105** 043004
[24] Ouchi T *et al* 2011 *Phys. Rev. Lett.* **107** 053401
[25] LaForge A C *et al* 2014 *Sci. Rep.* **4** 3621
[26] Ovcharenko Y *et al* 2014 *Phys. Rev. Lett.* **112** 073401
[27] Kochur A G, Sukhorukov V L, Dudenko A J and Demekhin P V 1995 *J. Phys. B: At. Mol. Opt. Phys.* **28** 387
[28] Simons R L and Kelly H P 1980 *Phys. Rev.* A **22** 625–9
[29] Amusia M Y, Lee I S and Kilin V A 1992 *Phys. Rev.* A **45** 4576–87
[30] Zeng J L, Liu P F, Xiang W J and Yuan J M 2013 *J. Phys. B: At. Mol. Opt. Phys.* **46** 215002
[31] Pindzola M S and Griffin D C 1987 *Phys. Rev.* A **36** 2628–32
[32] Pradhan A K and Nahar S N 2011 *Atomic Astrophysics and Spectroscopy* (New York: Cambridge University Press)
[33] Schneider T, Chocian P L and Rost J M 2002 *Phys. Rev. Lett.* **89** 073002

[34] Hikosaka Y, Lablanquie P, Penent F, Selles P, Kaneyasu T, Shigemasa E, Eland J H D and Ito K 2009 *Phys. Rev.* A **80** 031404
[35] Hoszowska J *et al* 2009 *Phys. Rev. Lett.* **102** 073006
[36] Grum-Grzhimailo A N and Kabachnik N M 2004 *J. Phys. B: At. Mol. Opt. Phys.* **37** 1879
[37] Kabachnik N M, Sazhina I P and Ueda K 1999 *J. Phys. B: At. Mol. Opt. Phys.* **32** 1769
[38] Ueda K, Shimizu Y, Chiba H, Kitajima M, Tanaka H, Fritzsche S and Kabachnik N M 2001 *J. Phys. B: At. Mol. Opt. Phys.* **34** 107
[39] Viefhaus J, Cvejanović S, Langer B, Lischke T, Prümper G, Rolles D, Golovin A V, Grum-Grzhimailo A N, Kabachnik N M and Becker U 2004 *Phys. Rev. Lett.* **92** 083001
[40] Viefhaus J, Grum-Grzhimailo A, Kabachnik N and Becker U 2004 *J. Electron Spectrosc. Relat. Phenom.* **141** 121–6
[41] Åberg T 1975 Two-photon emission, the radiative auger effect, and the double auger process *Atomic Inner-Shell Processes* ed B Crasemann vol I (New York: Academic) p 353
[42] Carlson T A and Krause M O 1966 *Phys. Rev. Lett.* **17** 1079–83
[43] Krause M O and Carlson T A 1966 *Phys. Rev.* **149** 52–8
[44] Cairns R B, Harrison H and Schoen R I 1969 *Phys. Rev.* **183** 52–6
[45] Wiel M V D and Wiebes G 1971 *Physica* **53** 225–55
[46] Saito N and Suzuki I H 1994 *Phys. Scr.* **49** 80
[47] Kammerling B, Krassig B and Schmidt V 1992 *J. Phys. B: At. Mol. Opt. Phys.* **25** 3621
[48] Saito N and Suzuki I H 1997 *J. Phys. Soc. Japan* **66** 1979
[49] Kanngießer B *et al* 2000 *Phys. Rev.* A **62** 014702
[50] Brünken S, Gerth C, Kanngießer B, Luhmann T, Richter M and Zimmermann P 2002 *Phys. Rev.* A **65** 042708
[51] Tamenori Y, Okada K, Tanimoto S, Ibuki T, Nagaoka S, Fujii A, Haga Y and Suzuki I H 2004 *J. Phys. B: At. Mol. Opt. Phys.* **37** 117
[52] Lablanquie P, Sheinerman S, Penent F, Hall R I, Ahmad M, Hikosaka Y and Ito K 2001 *Phys. Rev. Lett.* **87** 053001
[53] Viefhaus J, Braune M, Korica S, Reinkster A, Rolles D and Becker U 2005 *J. Phys. B: At. Mol. Opt. Phys.* **38** 3885
[54] Penent F, Palaudoux J, Lablanquie P, Andric L, Feifel R and Eland J H D 2005 *Phys. Rev. Lett.* **95** 083002
[55] Lablanquie P, Andric L, Palaudoux J, Becker U, Braune M, Viefhaus J, Eland J and Penent F 2007 *J. Electron Spectrosc. Relat. Phenom.* **156–158** 51–7
[56] Eland J H D, Linusson P, Hedin L, Andersson E, Rubensson J E and Feifel R 2008 *Phys. Rev.* A **78** 063423
[57] Palaudoux J, Lablanquie P, Andric L, Ito K, Shigemasa E, Eland J H D, Jonauskas V, Kučas S, Karazija R and Penent F 2010 *Phys. Rev.* A **82** 043419
[58] Andersson E, Fritzsche S, Linusson P, Hedin L, Eland J H D, Rubensson J E, Karlsson L and Feifel R 2010 *Phys. Rev.* A **82** 043418
[59] Nakano M, Hikosaka Y, Lablanquie P, Penent F, Huttula S M, Suzuki I H, Soejima K, Kouchi N and Ito K 2012 *Phys. Rev.* A **85** 043405
[60] Hayaishi T, Murakami E, Morioka Y, Shigemasa E, Yagishita A and Koike F 1995 *J. Phys. B: At. Mol. Opt. Phys.* **28** 1411
[61] Kochur A, Sukhorukov V and Demekhin V 2004 *J. Electron Spectrosc. Relat. Phenom.* **137–140** 325–8
[62] Kreidi K *et al* 2008 *Phys. Rev.* A **78** 043422
[63] Murakami E, Hayaishi T, Yagishita A and Morioka Y 1990 *Phys. Scr.* **41** 468
[64] Lablanquie P, Sheinerman S, Penent F, Hall R I, Ahmad M, Aoto T, Hikosaka Y and Ito K 2002 *J. Phys. B: At. Mol. Opt. Phys.* **35** 3265
[65] Sheinerman S A 1994 *J. Phys. B: At. Mol. Opt. Phys.* **27** L571
[66] Sheinerman S A 1998 *J. Phys. B: At. Mol. Opt. Phys.* **31** L361
[67] Koike F 1994 *Phys. Lett.* A **193** 173–8
[68] Sheinerman S, Lablanquie P, Penent F, Hikosaka Y, Kaneyasu T, Shigemasa E and Ito K 2010 *J. Phys. B: At. Mol. Opt. Phys.* **43** 115001
[69] Gerchikov L and Sheinerman S 2011 *Phys. Rev.* A **84** 022503
[70] Sheinerman S, Linusson P, Eland J H D, Hedin L, Andersson E, Rubensson J E, Karlsson L and Feifel R 2012 *Phys. Rev.* A **86** 022515
[71] Azuma Y, Hasegawa S, Koike F, Kutluk G, Nagata T, Shigemasa E, Yagishita A and Sellin I A 1995 *Phys. Rev. Lett.* **74** 3768–71
[72] Wehlitz R, Huang M T, Berrington K A, Nakazaki S and Azuma Y 1999 *Phys. Rev.* A **60** R17–20
[73] Berrington K and Nakazaki S 1998 *J. Phys. B: At. Mol. Opt. Phys.* **31** 313
[74] Pindzola M S, Robicheaux F and Colgan J 2005 *Phys. Rev.* A **72** 022709
[75] Rinn K, Gregory D C, Wang L J, Phaneuf R A and Müller A 1987 *Phys. Rev.* A **36** 595–8
[76] Hitchcock A P, Lablanquie P, Morin P, Lizon A, Lugrin E, Simon M, Thiry P and Nenner I 1988 *Phys. Rev.* A **37** 2448–66
[77] Kaneyasu T, Hikosaka Y, Lablanquie P, Penent F, Andric L, Gamblin G, Eland J H D, Tamenori Y, Matsushita T and Shigemasa E 2008 *Phys. Rev. Lett.* **101** 183003
[78] Eland J, Linusson P, Hedin L, Andersson E, Rubensson J E and Feifel R 2010 *Chem. Phys. Lett.* **485** 21–5
[79] Eland J H D, Hochlaf M, Linusson P, Andersson E, Hedin L and Feifel R 2010 *J. Chem. Phys.* **132** 014311
[80] Eland J H D *et al* 2010 *J. Chem. Phys.* **132** 104311
[81] Ågren H 1981 *J. Chem. Phys.* **75** 1267–83
[82] Tarantelli F, Sgamellotti A and Cederbaum L S 1992 *Applied Many-Body Methods in Spectroscopy and Electronic Structure* ed D Mukherjee (New York: Plenum)
[83] Müller A *et al* 2015 *Phys. Rev. Lett.* **114** 013002
[84] Colgan J, Emmanouilidou A and Pindzola M S 2013 *Phys. Rev. Lett.* **110** 063001
[85] Ogurtsov G N, Flaks I P and Avakyan S V 1971 *Sov. Phys.—Tech. Phys.* **15** 1656
[86] Rudd M E, Fastrup B, Dahl P and Schowengerdt F D 1973 *Phys. Rev.* A **8** 220–5
[87] Žitnik M *et al* 2016 *Phys. Rev.* A **93** 021401
[88] Chen M H 1991 *Phys. Rev.* A **44** 239–42
[89] Inhester L, Groenhof G and Grubmüller H 2013 *J. Chem. Phys.* **138** 164304
[90] Afrosimov V V, Gordeev Y S, Zinoviev A N, Korotkov A A and Shergin A P 1977 *Proc. 10th ICPEAC (Paris)* p 184
[91] Eland J H D, Squibb R J, Mucke M, Zagorodskikh S, Linusson P and Feifel R 2015 *New J. Phys.* **17** 122001
[92] Schirmer J, Trofimov A B and Stelter G 1998 *J. Chem. Phys.* **109** 4734–44
[93] Ivanov L N, Safronova U I, Senashenko V S and Viktorov D S 1978 *J. Phys. B: At. Mol. Opt. Phys.* **11** L175
[94] Simons R L and Kelly H P 1979 *Phys. Rev.* A **19** 682
[95] Safronova U I and Senashenko V S 1977 *J. Phys. B: At. Mol. Opt. Phys.* **10** L271
[96] Cederbaum L S, Domcke W, Schirmer J and Niessen W V 1986 Correlation effects in the ionization of molecules: breakdown of the molecular orbital picture *Advances in Chemical Physics* (New York: Wiley) pp 115–59
[97] Kolorenč P, Averbukh V, Gokhberg K and Cederbaum L S 2008 *J. Chem. Phys.* **129** 244102
[98] Averbukh V and Cederbaum L S 2005 *J. Chem. Phys.* **123** 204107
[99] Ghosh A and Vaval N 2014 *J. Chem. Phys.* **141** 234108

[100] Schnorr K *et al* 2015 *J. Electron Spectrosc. Relat. Phenom.* **204** 245–56
[101] Öhrwall G *et al* 2004 *Phys. Rev. Lett.* **93** 173401
[102] Santra R, Zobeley J and Cederbaum L S 2001 *Phys. Rev.* B **64** 245104
[103] Averbukh V and Cederbaum L S 2006 *Phys. Rev. Lett.* **96** 053401
[104] Ghosh A, Pal S and Vaval N 2014 *Mol. Phys.* **112** 669–73
[105] Sisourat N, Kryzhevoi N V, Kolorenč P, Scheit S, Jahnke T and Cederbaum L S 2010 *Nat. Phys.* **6** 508–11
[106] Sisourat N, Sann H, Kryzhevoi N V, Kolorenč P, Havermeier T, Sturm F, Jahnke T, Kim H K, Dörner R and Cederbaum L S 2010 *Phys. Rev. Lett.* **105** 173401
[107] Stumpf V, Kolorenč P, Gokhberg K and Cederbaum L S 2013 *Phys. Rev. Lett.* **110** 258302
[108] Gokhberg K, Kolorenc P, Kuleff A I and Cederbaum L S 2014 *Nature* **505** 661
[109] Trinter F *et al* 2014 *Nature* **505** 664–6
[110] Cherkes I and Moiseyev N 2011 *Phys. Rev.* B **83** 113303
[111] Bande A 2013 *J. Chem. Phys.* **138** 214104
[112] Pont F M, Bande A and Cederbaum L S 2013 *Phys. Rev.* B **88** 241304
[113] Averbukh V, Müller I B and Cederbaum L S 2004 *Phys. Rev. Lett.* **93** 263002
[114] Lauer S, Liebel H, Vollweiler F, Schmoranzer H, Lagutin B M, Demekhin P V, Petrov I D and Sukhorukov V L 1999 *J. Phys. B: At. Mol. Opt. Phys.* **32** 2015
[115] Stoychev S D, Kuleff A I, Tarantelli F and Cederbaum L S 2008 *J. Chem. Phys.* **129** 074307
[116] Demekhin P V, Chiang Y C, Stoychev S D, Kolorenč P, Scheit S, Kuleff A I, Tarantelli F and Cederbaum L S 2009 *J. Chem. Phys.* **131** 104303
[117] Gnodtke C, Saalmann U and Rost J M 2009 *Phys. Rev.* A **79** 041201
[118] Gorkhover T *et al* 2012 *Phys. Rev. Lett.* **108** 245005
[119] Garibay A C, Saalmann U and Rost J M 2015 *J. Phys. B: At. Mol. Opt. Phys.* **48** 174003
[120] Buchta D *et al* 2013 *J. Chem. Phys.* **139** 084301
[121] Marr G and West J 1976 *At. Data Nucl. Data Tables* **18** 497–508